Growth of Carbon Nanotubes from Heterometallic Palladium and Copper Catalysts

Justin P. O'Byrne[†,ϕ], Zhonglai Li[†,ϕ], Joseph M. Tobin[†], J. Andreas Larsson[‡], Peter Larsson[ð], Rajeev Ahuja[ð] and Justin D. Holmes[†,ϕ*].

[†]Materials and Supercritical Fluid Group, Department of Chemistry and the Tyndall National Institute, University College Cork, Cork, Ireland. [ϕ]Centre for Research on Adaptive Nanostructures and Nanodevices (CRANN), Trinity College Dublin, Dublin 2, Ireland. [‡]Theory Group, Tyndall National Institute, University College Cork, Lee Maltings, Prospect Row, Cork, Ireland. [ð]Condensed Matter Theory Group, Department of Physics & Materials Science, Uppsala University, P. O. Box 530, SE-751 21 Uppsala, Sweden

*To whom correspondence should be addressed Tel: +353 (0)21 4903608; Fax: +353 (0)21 4274097; Email: j.holmes@ucc.ie

Abstract

Bamboo-structured carbon nanotubes (BCNTs) were synthesized using MgO-supported Pd and Cu catalysts, doped with either Mo or W, by the catalytic chemical vapor decomposition of methane. No nanotubes were observed to grow from the catalysts in the absence of the dopant metals. Additionally, the level of dopant in the catalysts was found to strongly affect the morphology of carbon produced. Amorphous carbon was generated on a 10 wt. % Cu/5

wt. % W (2:1) catalyst, whilst BCNTs were produced on 20 wt. % Cu/5 wt. % W (4:1) and a 30 wt. % Cu/5 wt. % W (6:1) catalysts. A pure Pd catalyst produced carbon nanofibres (CNFs), whilst BCNTs were able to grow from Pd/Mo catalysts. Density functional theory simulations show that the composite Cu/W and Pd/Mo bimetallic particles which generated BCNTs have similar binding energies to carbon, and comparable to metals such as Fe, Co and Ni which are traditionally used to grow CNTs by chemical vapor deposition.

Introduction

Carbon nanotubes (CNTs) have attracted tremendous attention due to their extraordinary electrical and mechanical properties[1]. Applications of these one dimensional nanostructures include supercapicitors[2] and potential constituents in beyond Si CMOS scaling[3], which have been proposed and demonstrated in recent years. In addition, hetero- and hybrid-structures based on CNTs have shown huge potential for energy storage[4], the reinforcement of polymers[5], as well as photovoltaic cells and gas sensors[6]. A comprehensive review of carbon nanotubes has been reported by Dresselhaus *et al*[7]. Fundamental conditions that need to be controlled for CNT growth include reaction temperature as well as nanoparticle size and distribution[8]. However, oversimplification of the CNT formation process is misleading. The catalyst nanoparticle must crack the carbon source and support the resulting species[9]. The nanoparticle must also bind strongly enough with carbon in order to support the growth of a nanotube. Cu is not a traditional catalyst for growing CNTs as its binding strength to carbon is not large enough to support the dangling bonds of a growing CNT[10]. This inability to support CNT growth is in part due to the filled 3d orbital of Cu, which does not allow efficient orbital overlap with the hydrocarbon molecule. Fe, Co and Ni have partially filled 3d orbitals which allow the dissociation of the hydrocarbon molecules, as the molecule can donate electron density to the metal. This interaction along with “back-donation” from the

metal into the unoccupied orbitals in the hydrocarbon forms the basis for efficient carbon source cracking and support[11].

Density functional theory (DFT) calculations provide accurate models for the binding of CNTs to nanoparticles, which can be analyzed for "traditional" and other potential catalysts for CNT growth[12]. Here we report the use of DFT calculations to interpret our experimental observations on the growth of carbon nanostructures from Cu/W and Pd/Mo heterometallic clusters. We also compare our findings with data previously reported for CNTs grown for both active (Fe, Co and Ni) and non active (Au and Cu) [10-11] catalysts.

Experimental

Catalyst Preparation. The MgO support was prepared by the decomposition of $Mg_2(OH)_2CO_3$ at 450 °C for 6 hr in a furnace. Aqueous solutions of the metal (Pd and Cu) nitrates, ammonium molybdates and ammonium tungstenates were mixed with 2 g of MgO support, sonicated for 1 hr, dried in air and calcined at 500 ºC. For the detailed synthesis of the Cu/Mo catalyst refer to reference[10]. An aqueous solution of palladium (II) nitrate (0.126 g) was mixed with the MgO support to form the 5 % Pd on MgO catalyst. The Pd/Mo catalyst was formed by mixing $Pd(NO_3)_2.2H_2O$ and $(NH_4)Mo_6O_{24}.H_2O$ with the MgO support with Pd:Mo weight ratios of 4:1, 5:5 and 5:10 with respect to MgO. The Cu/W catalyst was formed by impregnating the MgO support with aqueous solutions of $Cu(NO_3)_2.6H_2O$ and $(NH_4)_{10}W_{12}O_{41}.5H_2O$ to form 10 % Cu / 5 % W, 20 % Cu / 5 % W and 30 % Cu / 5 % W. The mixture was sonicated for 1 hr and dried overnight. In all cases the dried powders were sintered at 500 °C for 6 h to produce the catalyst. The metal content of the catalyst was recorded as a weight percent with regard to the MgO support.

Chemical Vapor Deposition of Carbon. Carbon nanostructures were synthesized by the metal catalyst assisted CVD of methane. 0.3 g of the catalyst/MgO powder was placed in a quartz tube in the middle of a furnace and heated to 900 °C in a reducing atmosphere H_2/Ar (20/180 mL min^{-1}) for 30 min. After the catalyst activation, methane was introduced in the reaction chamber (flow rate of 100 mL min^{-1}) for 60 min and the system was allowed to cool to room temperature. The as-obtained material was treated with 3 M HNO_3 and rinsed with water to remove nanotubes from the metal catalyst and MgO support.

Characterization. Transmission electron microscopy (TEM) was performed on a Jeol 2000 FX and a Jeol 2100 operating at 120 kV or 200kV. Samples for TEM analysis were prepared in ethanol and deposited onto Cu or Ni grids. Raman spectra were recorded on a Renishaw 1000 Raman system in an ambient atmosphere using a 5 mW He-Ne laser (λ = 514.5 nm) and a CCD detector.

Theoretical Details. We have performed full geometry optimization DFT calculations of Cu/W and Pd/Mo particles of different compositions to determine their ability to stabilize and support the growing end of a CNT. We have computed a (5,0) SWNTs binding energy to a M_{13} metal cluster (M = Cu, Pd, W, Mo, and Cu/W and Pd/Mo composite particles), which in a model system that has been proven to correctly predict the trends in bonding[10, 13]. The resulting binding energies are compared to Fe, Co, Ni and Cu/Mo clusters of these previous reports. All calculations were made using the generalized gradient approximation (GGA) exchange and correlation potential by Perdew-Burke-Ernzenhof[14] [PBE], utilizing the polarized valence triple-ζ (TZVP) basis set[15] and relativistic effective core potentials (ECPs) for Cu, Pd, W and Mo[16], as implemented in the Turbomole suite of programs[17].

Results and Discussion

Carbon Nanofiber and Carbon Nanotube Synthesis

No nanotubes were grown by the CVD of methane over both pure MgO-supported Pd and Cu catalysts at a temperature of 900 ºC. Figure 1 shows carbon nanofibers synthesized from a pure Pd catalyst. The Pd nanoparticles under these reaction conditions crack the methane source which results in carbon nanofiber (CNF) formation. Without the addition of a dopant, the catalyst could not support carbon nanotube growth. In the case of Pd, we believe the nanoparticle becomes saturated with carbons, which are released by forming stacked graphitic plates. The Raman spectrum shown in Figure 2 for the carbon fibers show that there is some degree of graphitization, indicating some C-C bond formation. However, under these reaction conditions the Pd catalyst cannot support CNT formation as the Pd – carbon binding strength is too weak to support nanotube formation, as calculated and shown in Table 1.

Figure 3 shows TEM images of BCNTs synthesized by the CVD of methane over an MgO-supported Pd/Mo catalyst. The addition of Mo results in the binding of the nanoparticle to the carbon nanostructures. In the case of the Pd/Mo catalyst the binding strength of the nanoparticle is higher than that of Pd alone, resulting in the formation of a graphitic cap around the nanoparticles. As this carbon layer becomes bigger the nanoparticle deforms and becomes elongated, resulting in the formation of a chamber and the beginning of BCNT formation[18]. Whilst the Pd/Mo catalyst binds more strongly to the carbon shell compared to the Pd catalyst, see Table 1, the surface energy of the particle increases as it deforms during growth. When the surface energy is too high and cannot be compensated by binding to the graphitic layers, the catalytic nanoparticle returns to its minimum surface energy (roughly spherical) shape. This effect has been reported by Helveg *et al* in their study about Ni

catalysts for CNT growth[19]. Lin *et al.* have previously shown by *in-situ* TEM, the elongation and relaxation of Ni nanoparticles to form bamboo-compartments within CNTs[18]. As with these previous reports, upon retraction of the Pd/Mo nanoparticle to its spherical shape, the surface of the catalyst particle again becomes covered by graphitic layers. The continuous deformation and relaxation of Pd/Mo nanoparticles results in the growth of BCNTs. Raman analysis shows that the BCNTs grown from the Pd/Mo catalysts show higher levels of graphitization compared to the Pd grown CNFs, see Figure 2. Superior graphitization in the BCNTs would be expected due to fewer atom dislocations compared to layers present in the fibers.

Recently, Cu nanoparticles, supported on Si wafers, were used as catalysts for the production of single walled nanotubes (SWNTs)[20]. We previously reported the growth of BCNTs from MgO-supported Cu/Mo catalysts by the CVD of methane at 900 °C[10]. However, we have been unable to generate carbon nanostructures using MgO-supported Cu catalysts under these reaction conditions. Raman analysis of the carbon products generated from the Cu/W catalysts show the extent of graphitization in the samples (see Figure 4). Figure 5(a) shows a TEM image of a carbon product, with seemingly little structure, generated from a 10 wt. % Cu/5 wt. % W catalyst (2:1). Raman analysis of the same carbon product revealed a G-band (1591 cm^{-1}) which is indicative of the formation of graphene layers[21]. This peak when related to the D-band peak at 1325 cm^{-1} (I_D/I_G = 2) suggests a highly defective graphene structure. As the ratio of Cu to W was changed from 2:1 to 4:1, *i.e.* 20 wt. % Cu/5 wt. % W, BCNTs were observed to form. The formation of amorphous carbon over BCNTs is due to the differences in the binding energies between the composite nanoparticles and carbon, as shown by the values in table 1.

Figure 5(b) shows a TEM image of the carbon product formed from a 20 wt. % Cu/5 wt. % W catalyst, in particular showing the formation of BCNTs with average diameters of 24 nm. The I_D/I_G ratio in this case was 1.4, indicating a less defective structure than the 2:1 ratio. Figure 5(c) shows the carbon product formed from a 30 wt. % Cu/5 wt. % W catalyst, again showing the presence of BCNTs, with an average diameter of 23 nm. The I_D/I_G ratio for the 6:1 ratio was 1.23, which shows better graphitization for the BCNTs produced by this catalyst compared to the 4:1 Cu/W catalyst. The addition of a dopant to the Cu in the correct ratio alters the binding strength enough to allow the nanoparticles to support the dangling bonds of the open end of the growing CNT. The nanoparticle allows the formation of carbon-carbon bonds above the formation of metal carbides which occurs for Mo and W. The process of formation of the BCNTs is similar to the mechanism of formation for the Pd/Mo catalyst, by which the increase in the binding strength of the nanoparticle to carbon causes the nanoparticle to deform during chamber formation to form BCNTs by a similar mechanism.

Theoretical Results

Models of a small metal nanoparticle bound to a (5,0) SWNT segment (see Figure 6) have been used to calculate binding energies for different nanoparticles of different compositions (see Table 1), which we compare to the binding energies for traditional catalysts, M = Fe, Ni and Co, that are all slightly larger than the (5,0) SWNT dangling bond energy of 2.76 eV[12-13] using PBE/TZVP[14].

As can be seen in Table 1, the binding energies for the Cu_{13} and Pd_{13} clusters are lower than the carbon dangling bond energy of the (5,0) tube, while the binding energies for Mo_{13} and W_{13} are considerably higher. Herein, we compare relative theoretical binding energies to our observed results. Researchers have shown that the (5,0)-M_{13} complex consistently

reproduces the results of the more realistic (10,0)-M_{55} and (5,5)-M_{55} complexes, and can thus be used with confidence to explain metal-carbon binding strengths[10, 13]. Other groups have used graphene sheets[19], and even just benzene-like structures bound to the metal with one or two of its carbon atoms[22], to calculate metal-carbon binding energies to good effect. But such models would be less suitable when studying doping and alloying of the catalyst particles. Both Pd and Cu metal cluster scenarios agree with our experimental findings since all of these metals have been found to be non-active catalysts for CNT growth on their own. Pd_{13} displays a larger binding energy than Cu_{13}, which complies with Pd being an active catalyst for the growth of carbon nanofibers, *i.e.* Pd can decompose the carbon feed-stock at reasonable temperatures, but cannot support the hollow structure of a CNT. In contrast, our calculations show that Cu/W and Pd/Mo composite particles have binding energies in the same range as M = Fe, Co, and Ni. We have shown previously that only dopant atoms that are directly involved in binding to the CNT change the composite particle binding energy considerably[10], thus we only consider such cases in the present study. We find that replacing only one metal atom bound to the CNT (Cu by W, or Pd by Mo) can result in a suitably increased binding energy compared to the undoped Cu and Pd particles. This is seen for the $M'M_{12}$-top, and the M'_8M_5-top composite nanoparticles, and is more pronounced for the W doping of Cu than for the Mo doping of Pd. These results agree well with our experimental finding that lower ratios of Cu/W produce CNTs compared to Pd/Mo.

Metal-graphene interactions exhibit similar trends of binding strengths. Cu[23] and Pd interact weakly with graphene when compared with Ni and Co[24] due to their filled d-orbitals. The d-orbital model predicts stronger binding with decreasing occupation of the d band., therefore W would interact more strongly with graphene than Mo as it has fewer valence d electrons[25]. Pd is predicted to interact with graphene stronger than Cu[24] which corresponds to our

calculations, see Table 1. The interaction occurs predominantly with the π-orbital in the graphene interacting with the d orbitals in the metal, forming a dative bond. Comparing this model of metal-graphene interaction to the edge of the nanoparticle with a layer of carbon formed around it in the chamber of a BCNT, it is possible to further explain the growth mechanism involved in BCNT formation. An increased interaction of metal with graphene leads to a stabilized nanoparticle surface, as the carbon layer grows the nanoparticle deforms to maintain this stability until such a point where the energy cost from being elongated is more than the energy gain from being bound to the graphene layer. At the point where the nanoparticle cannot be stabilized and the chamber forming process repeats.

Adding a dopant to 'non-traditional' catalysts for nanotube growth can therefore bring these catalysts within the binding energy range of 'traditional' CNT catalysts. This is the basic "Goldilocks" hypothesis; if the binding strength is too weak the catalyst nanoparticle will not support the hollow carbon product and thus will be unable to support CNT growth. However, if the binding strength is too strong the carbon will simply form a metal carbide and the catalyst will become poisoned with carbon. The binding energies need to be within a certain range to firstly crack the feedstock gas and support the carbon species formed, but also support the hollow nanotube product generated. When these conditions are met, more carbon which has been cracked by the catalyst particle can be allowed to join the open growing end. This is fulfilled by Fe, Co and Ni, but not by Au and Cu, while Pd was found to be a border-line case[13a]. Transition metals such as W and Mo have been investigated for the growth of CNTs but their binding strengths to carbon are too strong and will form carbides.

Conclusions

We report the synthesis of CNTs and CNFs using novel heterometallic catalysts by CVD. The investigation of novel catalysts will be important for the future development of carbon nanotubes. The catalysts we used have previously shown no CNT forming capacity under these reaction conditions, with doping however, we have synthesized nanotubes from these metals. We have elucidated the mechanism for BCNT growth from the results obtained. As the growth mechanism of CNT formation becomes more understood, ways of tailoring the catalyst to form specific nanotubes with tunable properties will become prevalent. We believe the surface energy of a catalytic nanoparticle is stabilized by the formation of a graphene cap; as this cap increases in size due to the addition of more cracked carbon species, the nanoparticle changes shape in order to maximize this effect. As the graphene layer grows the nanoparticle elongates until the energy gain from being bonded to the carbon is less than the energy gained from being in its minimum surface energy state, *i.e.* a nearly spherical shape. CNTs have incredible potential for the development of beyond CMOS scaling. The catalysts' role in the formation of distinct tube diameter has been well documented[26], and to a lesser extent, the effect of the catalyst on the formation of distinct chiralities has been seen for Co-Mo catalysts[27].

Acknowledgements

The authors acknowledge financial support from CRANN/SFI (Grant 08/CE/I1432), the Tyndall National Access Programme (NAP Project 108), and the Swedish Research Council. This research was also enabled by the Higher Education Authority Program for Research in Third Level Institutions (2007-2011) via the INSPIRE programme.

Reference

1. (a) Dresselhaus, M.; Avouris, P., Carbon nanotunes, Synthesis, structure, properties and applications. *Springer ISBN 3540410864* **2001**; (b) Ebbesen, T. W.; Lezec, H. J.; Hiura, H.; Bennett, J. W.; Ghaemi, H. F.; Thio, T., Electrical conductivity of individual CNTs. *Nature* **1996,** *382*, 54.

2. Du, C.; Yeh, J.; Pan, N., High power density supercapicitors using locally aligned CNT electrodes. *Nanotechnology* **2005,** *16*, 350.

3. (a) Martel, R.; Derycke, V.; Lavoie, C.; Appenzeller, J.; Chan, K. K.; Tersoff, J.; Avouris, P., Ambipolar Electrical Transport in Semiconducting SWNTs. *Phys. Rev. Lett.* **2001,** *87* (25), 256805-1; (b) Seidel, R. V.; Graham, A. P.; J.;, K.; Rajasekharan, B.; Duesberg, G. S.; Liebau, M.; Unger, E.; Kreupl, F.; Hoenlein, W., Sub 20nm Short Channel CNT Transistors. *Nano Letters* **2005,** *5* (1), 147.

4. Reddy, A. L. R.; Shailumon, M. M.; Gowda, S. R.; Ajayan, P. M., Coaxial MnO2/CNT array electrodes for high performance Li Batteries. *Nano Lett* **2008,** *DOI: 10.1021/nl803081j*

5. Ci, L.; Suhr, J.; Pushparaj, V.; Zhang, X.; Ajayan, P. M., Continuous CNT Reinforced composites. *Nano Lett* **2008,** *8* (9), 2762.

6. Endo, M.; Strano, M. S.; Ajayan, P. M., Potential Applications of CNTs. *Topics Appl. Physics* **2008,** *111*, 13-62.

7. Dresselhaus, M. S. D., G.;; Jorio, A., Unusual Properties and Structure of Carbon Nanotubes. *Annu. Rev. Mater. Res* **2004,** *34*, 247-248.

8. (a) Cheung, C. L.; Kurtz, A.; Park, H.; Lieber, C. M., Diameter-Controlled Synthesis of Carbon Nanotubes. *J. Phys. Chem. B* **2002,** *106*, 2429; (b) Nerushev, O. A.; Morjan, R.-E.; Ostrovskii, D. I.; Sveningsson, M.; Jönsson, M.; Rohmund, F.; Campbell, E. E. B., The

Temperature Dependence of Fe Catalysed Growth of CNTs on Si Substrates. *Physica B: Condensed Matter* **2002,** *323* (1-4), 51.

9. Brukh, R.; Mitra, S., Mechanism of CNT growth by CVD. *Chem. Phys. Lett.* **2006,** *424* (1-3), 126.

10. Li, Z.; Larsson, J. A.; Larsson, P.; Ahuja, R.; Tobin, J. M.; O'Byrne, J.; Morris, M. A.; Attard, G.; Holmes, J. D., Cu/Mo catalysts for the growth of CNTs. *J. Phys. Chem. C.* **2008,** *112*, 12201.

11. Dupuis, A.-C., The Catalyst in the CCVD of Carbon Nanotubes - A Review. *Progress in Materials Science* **2005,** *50* (8), 929-961.

12. Ding, F.; Bolton, K.; Rosén, A., Nucleation and Growth of Single-Walled Carbon Nanotubes: A Molecular Dynamics Study. *J. Phys. Chem. B.* **2004,** *108*, 17369-17377.

13. (a) Ding, F.; Larsson, P.; Larsson, J. A.; Ahuja, R.; Duan, H.; Rosén, A.; Bolton, K., The Importance of Strong Carbon−Metal Adhesion for Catalytic Nucleation of Single-Walled Carbon Nanotubes. *Nano Letters* **2008,** *8*, 463; (b) Larsson, P.; Larsson, J. A.; Ahuja, R.; Ding, F.; Yakobson, B. I.; Duan, H.; Rosén, A.; Bolton, K., Calculating Carbon Nanotube-catalyst Adhesion Strengths. *Phys. Rev. B* **2007,** *75*, 115419.

14. Perdew, J. P.; Burke, K.; Ernzerhof, M., *Phys. Rev. Lett.* **1996,** *77*, 3865.

15. Schäfer, A.; Huber, C.; Ahlrichs, R., bas. *J. Chem. Phys.* **1994,** *100*, 5829.

16. (a) Andrae, D.; Haeussermann, U.; Dolg, M.; Stoll, H.; Preuss, H., ECP1. *Theor. Chim. Acta.* **1990,** *77*, 123; (b) Dolg, M.; Wedig, U.; Stoll, H.; Preuss, H., ECP2. *J. Chem. Phys.* **1987,** *86* (866).

17. (a) Treutler, O.; Ahlrichs, R., TM1 Turbomole. *J. Chem. Phys.* **1995,** *102*, 346; (b) Arnim, M. v.; Ahlrichs, R., TM2 Turbomole. *J. Comp. Chem.* **1998,** *19*, 1746; (c) Eichkorn, K.; Treutler, O.; Öhm, H., ;; Häser, M.; Ahlrichs, R., TM3 Turbomole. *Chem. Phys. Lett.*

1995, *240*, 283; (d) Ahlrichs, R.; Bär, R.; Häser, M.; Horn, H.; Kölmel, C., TM4 Turbomole *Chem. Phys. Lett.* **1989,** *162*, 165.

18. Lin, M.; Tan, J. P. Y.; Boothroyd, C.; Loh, K. P.; Tok, E., S.;; Foo, Y. L., Dynamical Observation of Bamboo like CNT Growth. *Nano Lett* **2007,** *7* (8), 2234.

19. Helveg, S.; Lo´pez-Cartes, C.; Sehested, J.; Hansen, P. L.; Clausen, B. S.; Rostrup, J. R.; Abild-Pederson, F.; Nørskov, J. K., Atomic-Scale imaging of carbon nanofibre growth. *Nature* **2004,** *427*, 426-429.

20. Zhou, W.; Han, Z.; Wang, J.; Zhang, Y.; Jin, Z.; Sun, X.; Zhang, Y.; Yan, C.; Li, Y., Copper Catalyzing Growth of Single-Walled Carbon Nanotubes on Substrates. *Nano Lett* **2006,** *6* (12), 2987-2990.

21. Dresselhaus, M. S.; Dresselhaus, G.; Saito, R.; Jorio, A., Raman Spec of CNTs. *Physics Reports* **2004**.

22. Yazyev, O. V.; Pasquarello, A., Effect of Metal Elements in Catalytic Growth of Carbon Nanotubes. *Phys. Rev. Lett.* **2008,** *100*, 156102.

23. Karpan, V. M.; Giovannetti, G.; Khomyakov, P. A.; Talanana, M.; Starikov, A. A.; Zwierzycki, M.; van den Brink, J.; Brocks, G.; Kelly, P. J., Graphite and Graphene as Perfect Spin Filters. *Phys. Rev. Lett.* **2007,** *99*, 176602.

24. Giovannetti, G.; Khomyakov, P. A.; Brocks, G.; Karpan, V. M.; van den Brink, J.; Kelly, P. J., Doping Graphene with Metal Contacts. *Phys. Rev. Lett.* **2008,** *101*, 026803.

25. Wintterlin, J.; Bocquet, M.-L., Graphene on metal surfaces. *Surface Science* **2009,** *603*, 1841-1852.

26. Li, Y.; Kim, W.; Zhang, Y.; Rolandi, M.; Wang, D.; Dai, H., Growth of Single-Walled Carbon Nanotubes from Discrete Catalytic Nanoparticles of Various Sizes. *J. Phys. Chem. B.* **2001,** *105*, 11424-11431.

27. Bachilo, S. M.; Balzano, L.; Herrera, J. E.; Pompeo, F.; Resasco, D. E.; Weisman, R. B., Narrow (n,m)-Distribution of Single-Walled Carbon Nanotubes Grown Using a Solid Supported Catalyst. *J. Am. Chem. Soc.* **2003,** *125*, 11186-11187

Figures and Tables

Table 1. Metal Cluster – (5,0) SWNT binding energies (eV) per carbon atom at open end of carbon nanotube.

	M_{13}	M'_{13}	$M'M_{12}$ side	$M'M_{12}$ top	M'_8M_5 top
M=Cu[a], M'=W	2.29	3.93	2.38	2.99	2.87
M=Cu, M'=Mo[a]	2.29	3.63	2.35	2.90	2.99
M=Pd, M'=Mo	2.48	3.63	2.37	2.75	2.52

[a] values taken from ref. 14.

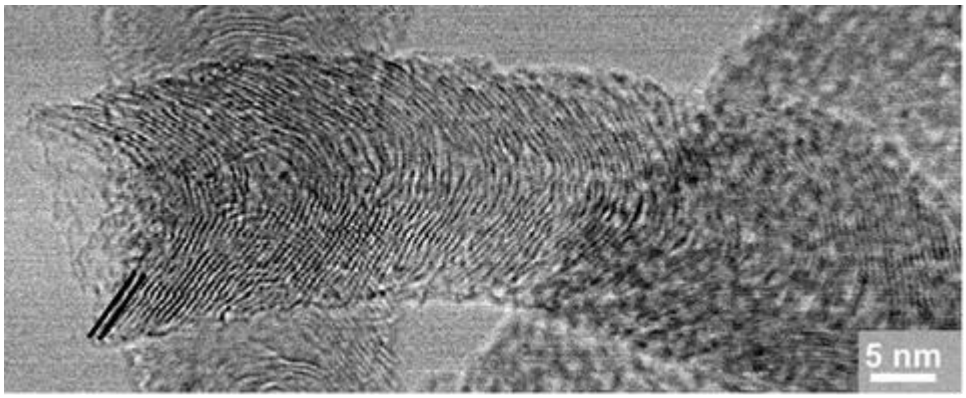

Figure 1. TEM images of carbon nanofibers grown by the CVD of methane over an MgO-supported Pd catalyst at 900 °C.

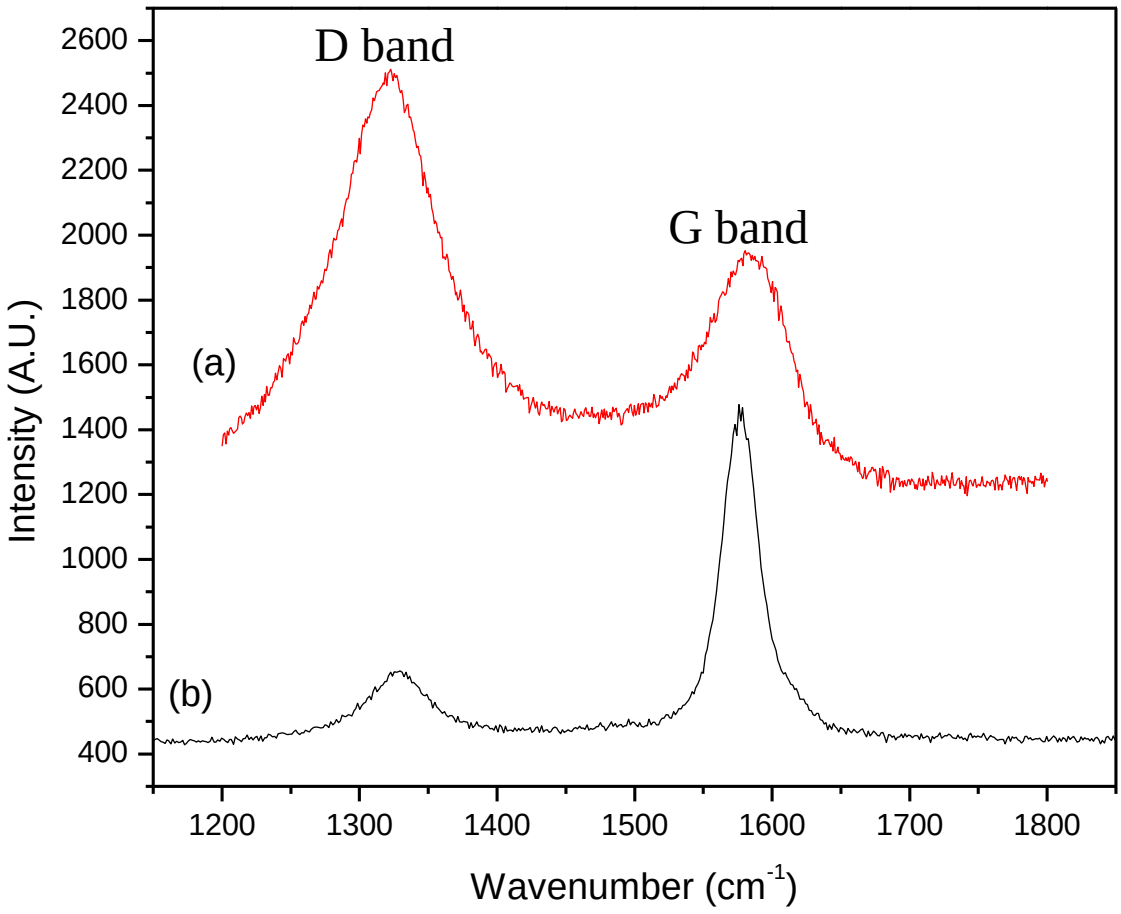

Figure 2. Raman spectra of (a) carbon fibers grown from an MgO-supported Pd catalyst and (b) BCNTs grown from MgO-supported Pd/Mo catalyst by the CVD of methane at a temperature of 900 °C. The peak at ~1380 cm^{-1} shows the D band which indicates the defect level in the sample. The peak at ~1590 cm^{-1} is the G band which shows the level of graphitization in the sample.

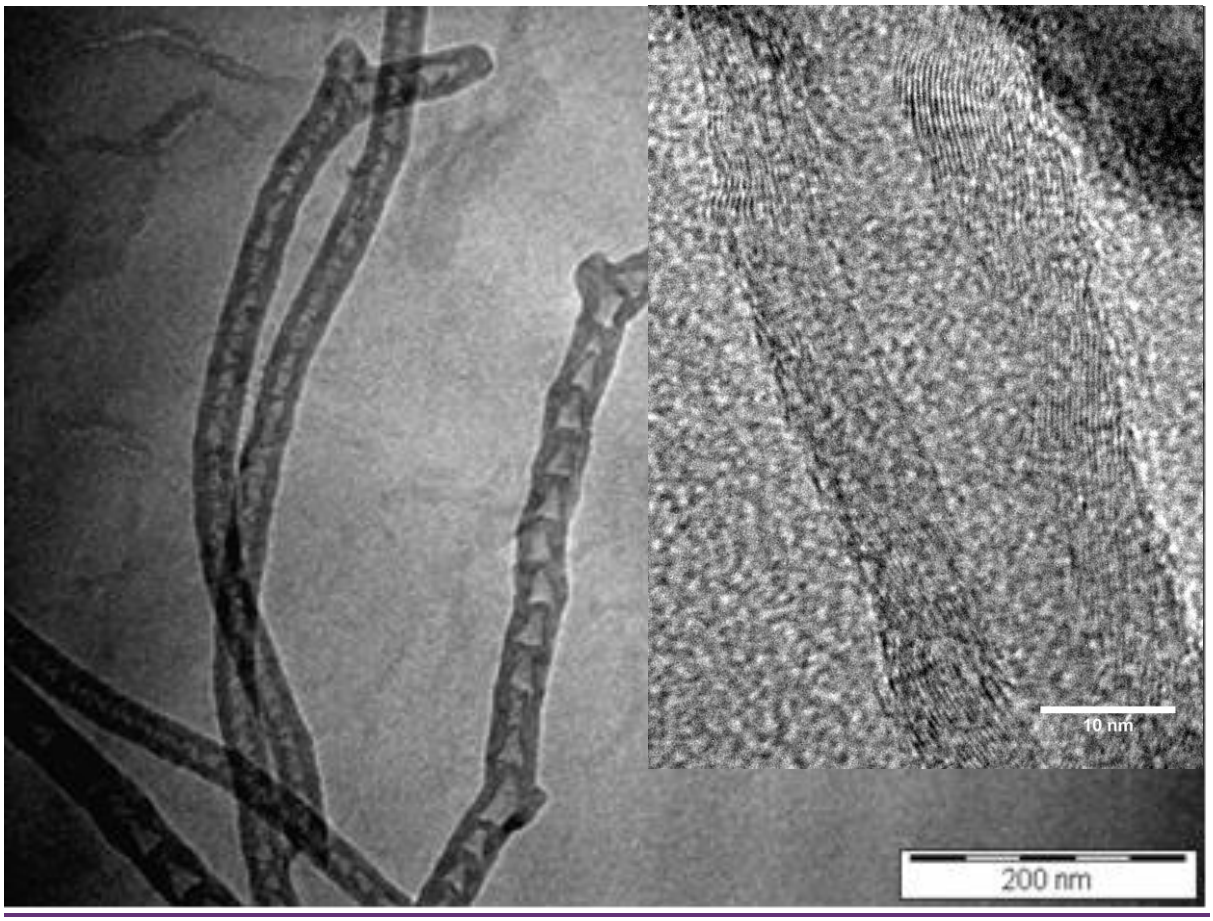

Figure 3. TEM images of BCNTs grown by the CVD of methane over an MgO-supported Pd catalyst at 900 °C.

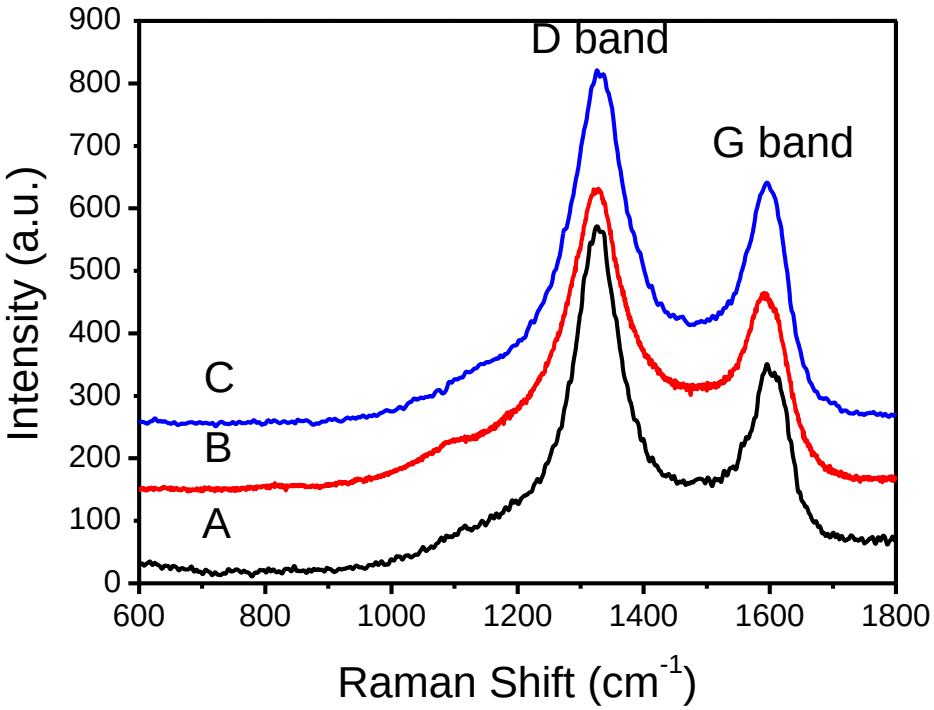

Figure 4. Raman spectra showing D band (~1325 cm^{-1}) and G band (~1591 cm^{-1}) of (A) 10 wt. % Cu / 5 wt. % W on MgO, (B) 20 wt. % Cu / 5 wt. % W on MgO, and (C) 30 wt. % Cu / 5 wt. % W on MgO.

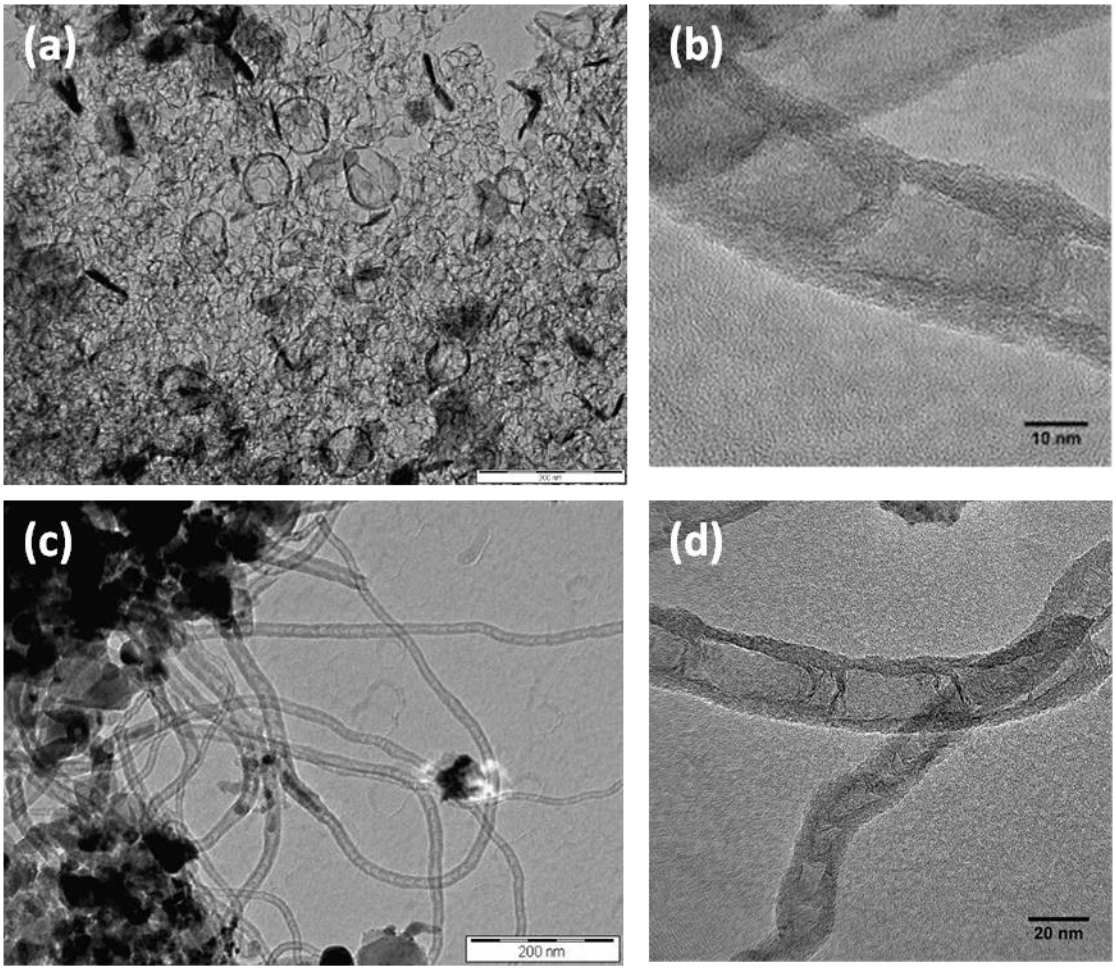

Figure 5. TEM images of BCNTs prepared on (a) 10wt%, (b) and (c) 20wt% and (d) 30wt% Cu-loaded over Cu-5 wt. % W/MgO catalyst at 900 ºC.

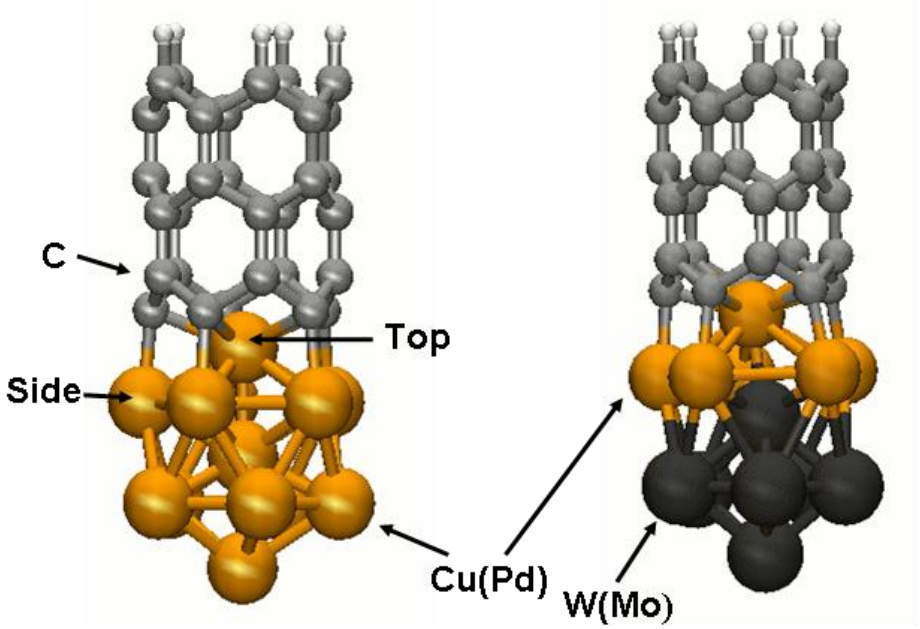

Figure 6. M_{13}-$C_{30}H_5$ models used for the calculation of binding strengths of a (5,0) SWNT bond to Cu_{13}, Pd_{13}, W_{13} and Mo_{13} nanoparticles, and W/Cu (Mo/Pd) composite particles by replacing either the "Side" or "Top" Cu (Pd) atoms with W (Mo), resulting in WCu_{12} ($MoPd_{12}$) clusters (left) and the W_8Cu_5 (Mo_8Pd_5) cluster (right).